JPET Fast Forward. Published on February 13, 2009 as DOI: 10.1124/jpet.108.150201
This article has not been copyedited and formatted. The final version may differ from this version.
JPET Fast Forward. Published on February 13, 2009 as DOI:10.1124/jpet.108.150201

Multifaceted approach to determine the antagonist molecular mechanism and interaction of ibodutant at the human tachykinin NK_2 receptor

Stefania Meini, Francesca Bellucci, Claudio Catalani, Paola Cucchi, Alessandro Giolitti, Paolo Santicioli, Sandro Giuliani

Departments of Pharmacology (SM, FB, CC, PC, PS, SG) and Drug Design (AG), Menarini Ricerche, Florence, Italy

Downloaded from jpet.aspetjournals.org at ASPET Journals on April 23, 2024

Copyright 2009 by the American Society for Pharmacology and Experimental Therapeutics.

JPET Fast Forward. Published on February 13, 2009 as DOI: 10.1124/jpet.108.150201
This article has not been copyedited and formatted. The final version may differ from this version.

Running title: Antagonist molecular mechanism at the human NK_2 receptor

Address correspondence to: Dr. Stefania Meini, Pharmacology Department, Menarini Ricerche S.p.A., via Rismondo 12A, Florence, Italy. Tel. 39 055 5680 736; FAX 39 055 5680 9954; *E-mail*: smeini@menarini-ricerche.it

Number of text pages: 29

Number of tables: 1

Number of figures: 7

Number of references: 41

Number of words in the Abstract: 234

Number of words in the Introduction: 519

Number of words in the Discussion: 1515

Abbreviations: NKA, neurokinin A; DMSO, dimethylsulfoxide; PBS, phosphate buffered saline; PI, phosphatidyl inositols; GPCRs, G protein coupled receptors.

Recommended section assignment: Cellular and Molecular

Downloaded from jpet.aspetjournals.org at ASPET Journals on April 23, 2024

JPET Fast Forward. Published on February 13, 2009 as DOI: 10.1124/jpet.108.150201
This article has not been copyedited and formatted. The final version may differ from this version.

Abstract

Ibodutant (MEN15596) is a tachykinin NK_2 receptor (NK_2R) antagonist currently under phase II clinical trials for irritable bowel syndrome. This study focuses on ibodutant pharmacodynamic profile at the human NK_2R and compares it with other two antagonists, nepadutant and saredutant. In functional experiments (phosphatidyl inositols accumulation) in CHO cells expressing the human NK_2R, ibodutant potency measured towards concentration-response curves to neurokinin A (NKA) as pK_B was 10.6 and its antagonism mechanism surmountable and competitive. In the same assay antagonism equilibration and reversibility experiments of receptor blockade indicated that ibodutant quickly attains equilibrium, and that reverts from receptor compartment in a slower manner. Kinetic properties of ibodutant were assessed through competitive binding kinetics experiments performed at [^{3}H]nepadutant and [^{3}H]saredutant binding sites. Determined K_{on} and K_{off} values indicated a fast association and slow dissociation rate of ibodutant at the different antagonist binding sites. Last, by radioligand binding experiments at some mutated human tachykinin NK_2Rs, the aminoacidic determinants crucial for the high affinity of ibodutant were identified at transmembrane (TM) level: C167 in TM4, I202 and Y206 in TM5, F270, Y266, and W263 in TM6, and Y289 in TM7. These results indicated an extended antagonist binding pocket in the TM portion of the receptor, which is conceived crucial for the TMs 3 and 6 arrangement, and leads to GPCR receptor activation. By combining these informations and molecular modeling the docking mode of ibodutant-human NK_2R complex is proposed.

Downloaded from jpet.aspetjournals.org at ASPET Journals on April 23, 2024

JPET Fast Forward. Published on February 13, 2009 as DOI: 10.1124/jpet.108.150201
This article has not been copyedited and formatted. The final version may differ from this version.

Introduction

G-protein coupled receptors (GPCRs) represent about 50% of current therapeutic targets. Antagonists for GPCR are so defined because of their capability to interfere with the ability of agonists in producing a given pharmacological response. The determination of the mechanism of action of an antagonist is one of the major pharmacological endeavour in drug discovery, and can be helpful to predict the antagonist properties in the therapeutic situation.

The tachykinin NK_2 receptor (NK_2R) is a seven transmembrane class A (rhodopsin-like) GPCR, which is preferentially activated by neurokinin A (NKA, HKTDSFVGLM-NH_2) leading to Gq/11 coupling and following activation of phospholipase C, thus producing inositol 3-phosphate and diacylglicerol (Almeida et al., 2004).

Antagonists for the tachykinin NK_2R are considered as potential innovating therapeutic drugs in different diseases and are currently under clinical development for irritable bowel syndrome, post-operative ileus, and depression disorders (Lecci and Maggi, 2003; Quartara and Altamura, 2006; Giuliani et al., 2008). Tachykinin NK_2 receptor antagonists presently in clinical trials are the nonpeptide saredutant (SR48968, Advenier et al., 1992), the glycosylated bicyclic peptide nepadutant (MEN11420, Catalioto et al., 1998a), and the more recently presented nonpeptide ibodutant (MEN15596, Cialdai et al. 2006; Giuliani et al., 2008).

Ibodutant belongs to a structurally distinct class of compounds in respect to the other previously discovered NK_2 antagonists. Structure-activity studies which led to the selection of this class of structures, and then of ibodutant, have been recently disclosed (Sisto et al., 2007; Fedi et al., 2007; Porcelloni et al., 2008).

The *in vitro* and *in vivo* pharmacological outline of the nonpeptide antagonist ibodutant have indicated its high affinity and selectivity for the human tachykinin NK_2R (pK_i 10.1) over the NK_1 (pK_i 6.1) and NK_3 subtypes (pK_i 6.4), as well as its antagonist potency in human (pK_B 9.2), guinea pig (pK_B 9.3), and minipig (pK_B 8.8) NK_2R smooth muscle preparations (Cialdai et al., 2006). In the anaesthetized guinea pigs, both after parenteral and oral administration, ibodutant potently blocks NK_2R-mediated colonic motility and bronchoconstriction (Cialdai et al., 2006).

Downloaded from jpet.aspetjournals.org at ASPET Journals on April 23, 2024

JPET Fast Forward. Published on February 13, 2009 as DOI: 10.1124/jpet.108.150201
This article has not been copyedited and formatted. The final version may differ from this version.

Aim of the current investigation is to provide clues on the exerted antagonism and the nature of the molecular interaction of ibodutant with the human tachykinin NK_2R, and to compare it along the study with the other two reference antagonists nepadutant and saredutant.

We used a recombinant cell system because of the paucity of available human tissue or cells which natively express this receptor. The concentration-dependent antagonism was evaluated towards the NKA-induced phosphatidyl inositol (PI) accumulation (as index of receptor-mediated phospholipase C activation). The kinetic properties of ibodutant were evaluated in terms of reversibility from the receptor compartment by measuring the recovery of the agonist functional response in the same assay. Then, in order to provide quantitative information on the association and dissociation rates of ibodutant, while not having the radiolabelled antagonist, competition kinetics were carried out with ibodutant by using the two structurally distinct radiolabelled antagonists nepadutant and saredutant. Last, by carrying out radioligand binding at some mutated human tachykinin NK_2Rs, the critical determinants for ibodutant high affinity are identified and, with the aid of receptor modeling, a model of this antagonist docked to the receptor is proposed.

Downloaded from jpet.aspetjournals.org at ASPET Journals on April 23, 2024

JPET Fast Forward. Published on February 13, 2009 as DOI: 10.1124/jpet.108.150201
This article has not been copyedited and formatted. The final version may differ from this version.

Methods

Chemicals

NKA was obtained by EspiKem (Florence, Italy). Nepadutant (MEN11420; (cyclo-{[Asn(β-D-GlcNAc)-Asp-Trp-Phe-Dpr-Leu]cyclo(2β-5β)}) (batch NEP L1/05) and ibodutant ([1-(2-phenyl-1R-{[1-(tetrahydropyran-4-ylmethyl)-piperidin-4-ylmethyl]-carbamoyl}-ethylcarbamoyl)-cyclopentyl]-amide) (batch L1/04) were synthesized in Lusochimica (Lomagna, Italy). Saredutant (SR48968, (S)-N-methyl-N[4-(4-acetylamino-4-phenylpiperidino)-2-(3,4-dichlorophenyl)butyl] benzamide) was a kind gift of Sanofi (Montpellier, France). [^{125}I]NKA (specific activity 2000 Ci·mmol^{-1}) was provided by Amersham Biosciences (Buckinghamshires, U.K.), [^{3}H]saredutant (specific activity 25.5 Ci·mmol^{-1}) (Emonds-Alt *et al.*, 1993) and *myo*-[1,2-^{3}H] inositol (specific activity 75 Ci·mmol^{-1}) by Perkin Elmer (Boston, MA, U.S.A.). [^{3}H]nepadutant (specific activity 30 Ci·mmol^{-1}) (Renzetti *et al.*, 1998) was synthesized by SibTech Inc. (Newington, CT, USA). All salts used were purchased from Merck and all other materials from Sigma. Peptidic ligands were dissolved in water, and nonpeptide ligands in DMSO up to 100 µM. All compounds were stored at -25°C.

Cells

Chinese hamster ovary (CHO-K1) cells stably expressing the human tachykinin NK_2R (provided by Dr. J.E. Krause, Washington University, School of Medicine, St Louis, MO) were cultured in α-modification essential Eagle's (αMEM) medium containing 10% foetal bovine serum (FBS, characterized, Cat. No. SH30071.03, HyClone, Utah, USA), 2 mM L-glutamine, and 1% of penicillin and streptomycin, and used for functional experiments.

Dihydrofolate reductase-(DHFR)-deficient CHO cell line CHO DUKX-B11 stably expressing the wild type or mutated human tachykinin NK_2R (provided by Drs. S. Zappitelli and L. Rotondaro, Menarini Biotech, Rome, Italy) were cultured as above but using dialysed FBS (dialyzed, Cat. No. SH30079.03, Hyclone, Utah, USA), and used for binding experiments.

Downloaded from jpet.aspetjournals.org at ASPET Journals on April 23, 2024

JPET Fast Forward. Published on February 13, 2009 as DOI: 10.1124/jpet.108.150201
This article has not been copyedited and formatted. The final version may differ from this version.

Measurement of phosphatidyl inositol (PI) accumulation

Cells were grown in 24-well tissue culture plates and labelled with *myo*-[^{3}H] inositol (0.5 ml/well, 1 µCi·ml^{-1}) in Iscove's modified Dulbecco's medium and Ham's F12 medium (1:1) containing 1% FBS and L-glutamine (2 mM). After 24 h different concentrations of NKA (1 nM – 100 µM) were incubated for 30 min at 37°C in the stimulation buffer (PBS without Ca^{2+} and Mg^{2+} 135 mM, HEPES 20 mM, $CaCl_2$ 2 mM, $MgSO_4$ 1.2 mM, EGTA 1 mM, glucose 11.1 mM, captopril 10 µM, BSA 0.05%) added with LiCl (25 mM) in the absence or in the presence of the indicated concentration of antagonist preincubated as indicated in the text. Total inositol phosphates levels were determined as previously described (Meini *et al.*, 2005). Determinations were in triplicate.

Membrane preparation and radioligand binding assay

Cells at confluence were rinsed with ice-cold PBS without Ca^{2+} and Mg^{2+}, collected and pelleted by centrifugation at 200 g, for 10 min at 4 °C. The cell pellet was suspended in Tris·HCl (50 mM), pH 7.4, containing bacitracin (0.1 mg·ml^{-1}), chymostatin (0.01 mg·ml^{-1}), leupeptin (5 µg·ml^{-1}) and thiorphan (10 µM) (buffer A), and homogenized with a Polytron (PT 3000, Kinematica). The homogenate was centrifuged at 25,000 g for 1 h at 4°C and the pellet was resuspended in the binding buffer composed of buffer A supplemented with 150 mM NaCl, 5 mM $MnCl_2$, and 0.1% BSA (binding buffer) to obtain 5 mg·ml^{-1} membrane protein concentration, and frozen immediately in 1 ml aliquots by immersion in liquid nitrogen, and there stored until use.

Binding assay was performed at room temperature in a final volume of 0.5 ml, and with a different incubation time according to the used radioligand: 30 min for [^{125}I]NKA and [^{3}H]saredutant, and 60 min for [^{3}H]nepadutant. Each radioligand was used at a concentration less than the calculated K_d value for the studied receptor (wild type or mutant) to give a bound less than 10% of the total added radioligand concentration, and a specific binding which represented approximately the 70-80 % of the total binding. Non-specific binding was defined as the amount of radiolabelled ligand bound in the presence of the appropriate unlabelled ligand (1 µM). Competing ligands were tested in a wide range of concentrations (1 pM – 10 µM). The final DMSO concentration in the assay was

Downloaded from jpet.aspetjournals.org at ASPET Journals on April 23, 2024

JPET Fast Forward. Published on February 13, 2009 as DOI: 10.1124/jpet.108.150201
This article has not been copyedited and formatted. The final version may differ from this version.

1% and did not affect radioligand binding. All incubations were terminated by rapid filtration through UniFilter-96 plates (Packard Instrument Company), pre-soaked for at least 2 h in polyethylenimine 0.3%, and using a MicroMate 96 Cell Harvester (Packard Instrument Company). The tubes and filters were then washed 5 times with 0.5 ml aliquots of Tris·HCl buffer (50mM, pH 7.4, 4°C). Filters were dried and soaked in Microscint 40 (50 μl in each well, Packard Instrument Company), and bound radioactivity was counted by a TopCount Microplate Scintillation Counter (Packard Instrument Company). Determinations were performed in duplicate.

Analysis of pharmacological data

All values in the text, tables or figures are mean and 95% confidence limits (95% c.l.), or mean ± s.e.mean of the given number of experiments (n).

Concentration-response curves in functional experiments were analyzed by sigmoidal nonlinear regression fit using the GraphPad Prism 4.0 program (San Diego, CA, U.S.A.) to determine the molar concentration of the agonist producing the 50% (EC_{50}) of its maximal effect (E_{max}) or the antagonist concentration producing the 50% inhibition of agonist response (IC_{50}).

In functional experiments (measuring the PI accumulation) agonist responses obtained either in the absence (control) or presence of antagonist were normalized towards the E_{max} of control NKA. The antagonist potency was expressed as apparent pK_B calculated from the equation:

pK_B = log [CR - 1] - log [antagonist concentration]

where the concentration-ratio (CR) is the ratio of equieffective concentrations (EC_{50}) of NKA in the presence and absence of antagonist (Kenakin, 1997). The nature of the antagonism was checked by means of Schild analysis.

All binding data were fitted by using GraphPad Prism 4.0 in order to determine the equilibrium dissociation constant (K_d) from homologous competition experiments, the ligand concentration inhibiting the radioligand binding of the 50% (IC_{50}) from heterologous competition experiments (performed with ibodutant), and kinetic parameters (K_{obs}, observed association rate constant; K_{off}, dissociation rate constant). K_d values were calculated as IC_{50} - [radioligand]. K_i

Downloaded from jpet.aspetjournals.org at ASPET Journals on April 23, 2024

JPET Fast Forward. Published on February 13, 2009 as DOI: 10.1124/jpet.108.150201
This article has not been copyedited and formatted. The final version may differ from this version.

values of ibodutant were calculated from IC_{50} using the Cheng-Prusoff equation ($K_i = IC_{50}/(1 + [radioligand]/K_d)$ according to the concentration and K_d of the used radioligand (Cheng and Prusoff, 1973).

Competition kinetic binding experiments between the antagonist radioligand ([^{3}H]nepadutant or [^{3}H]saredutant) and the unlabelled ibodutant as competitor were carried out as described by Motulsky and Mahan (1984) and more recently applied by Dowling and Charlton (2006). Briefly, association binding studies were carried out with the radioligand, in the absence or presence of different concentration of ibodutant: labelled and unlabelled ligand were add together and the binding of the labelled ligand was measured over the time. Association (K_{on} or K_3) and dissociation (K_{off} or K_4) rates for ibodutant were calculated by fitting (least squares) the data from the competition kinetic experiments with a two-component exponential curve, as detailed by Dowling and Charlton (2006; equation 3) by using graphPad Prism 4.0, keeping as fixed parameters the K_{on}, K_{off}, and concentration of the used radioligand and the total binding (B_{max} as c.p.m.) deriving from appropriate experiments as indicated in the text.

Modeling

The three-dimensional model for the transmembrane region of the human NK_2R was obtained starting from the crystal structure of bovine rhodopsin (Palczewski et al., 2000), as already described (Giolitti et al., 2002), further refined taking into account the recent crystal structure of β_2 adrenergic receptor (Rasmussen et al., 2007; Cherezov et al., 2007; Rosenbaum et al., 2007). Aminoacids side chains were optimized for contacts within the Sybyl molecular modelling software (v. 8.0, Tripos Inc., St. Louis, MO, USA). The starting ibodutant conformation was previously selected among a series of lower-energy conformers (structure 2 in Altamura et al., 2006), and the docking was performed manually.

Downloaded from jpet.aspetjournals.org at ASPET Journals on April 23, 2024

JPET Fast Forward. Published on February 13, 2009 as DOI: 10.1124/jpet.108.150201
This article has not been copyedited and formatted. The final version may differ from this version.

Results

Antagonist potency towards NKA induced PI accumulation in CHO cells expressing the human tachykinin NK_2R

The concentration-dependency of ibodutant antagonism was evaluated towards NKA-induced PI accumulation. NKA (0.1 nM – 10 μM) induced a concentration-dependent increase over the basal PI accumulation with an EC_{50} value of 4.1 nM (2.7 – 6.0, 95% c.l., n = 5) and E_{max} amounting to 6.5 ± 0.4 -fold over the basal response. Ibodutant (0.3 - 30 nM concentration range) was preincubated with cells 15 min before the agonist administration, and while *per se* did not modify the basal response, concentration-dependently shifted to the right the concentration response curve to NKA (Figure 1a). The Schild analysis of agonist concentration-response curves obtained in the absence (control) and in the presence of different concentrations of ibodutant indicated that the slope value of linear regression did not differ from unity (1.2, 0.9 – 1.3, 95% c.l.) (Figure 1b), consistent with a competitive antagonist behavior. The antagonist potency in terms of pK_B measured from Schild analysis as x-intecept was 10.3 (10.05 – 10.6, 95% c.l.) which did not diverge from the value measured from single experiments, being 10.6 ± 0.06 (n = 18).

Under the same experimental conditions the potency of nepadutant and saredutant was evaluated (Figure 2), and the estimated pA_2 values were 8.3 and 9.8, respectively.

Equilibration and reversibility of tachykinin NK_2R blockade

In order to confirm that the above experiments were performed under antagonist equilibrium conditions, a further set of experiments was performed in the PI accumulation assay in which ibodutant was left in contact with cells for a longer period of time before the agonist addition. Concentration-response curves to NKA were obtained after 15 or 60 min of pre-incubation with ibodutant at 2 nM concentration. This concentration was the same used for reversibility experiments (see below). Data were percentaged according to the basal values and maximal effect obtained with each conditions (15 and 60 min preincubation times). No differences were observed in NKA efficacy and EC_{50} or in the antagonism of ibodutant antagonism: the obtained concentration-ratio values were 89 ± 4 and 86 ± 5, after 15 and 60 min of antagonist contact time,

Downloaded from jpet.aspetjournals.org at ASPET Journals on April 23, 2024

JPET Fast Forward. Published on February 13, 2009 as DOI: 10.1124/jpet.108.150201
This article has not been copyedited and formatted. The final version may differ from this version.

respectively, yielding to overlapping pA_2 values of 10.6 (n=4, supplemental Figure 1).

The reversibility of ibodutant from receptor compartment was investigated and compared to that of the differently structured antagonists nepadutant and saredutant. Antagonists contact time was 15 min. The equieffective antagonists concentrations to inhibit the submaximal response induced by NKA (30 nM) were selected by means of antagonist inhibition curves which gave IC_{50} values of 0.22 nM (0.17 – 0.32, 95% c.l.) for ibodutant, 0.74 nM (0.56 – 0.98, 95% c.l.) for saredutant, and 33 nM (26 – 42, 95% c.l.) for nepadutant.

In reversibility functional experiments cells were preincubated 15 min with antagonists which inhibited the NKA (30 nM) induced PI accumulation: ibodutant (2 nM) by 88 ± 3%, nepadutant (300 nM) 87 ± 3% and saredutant (3nM) by 75 ± 2% (Figure 3). Therefore the agonist response was evaluated after washing with drug-free medium, which was renewed every 15 min (wash period) along a period of 3 hours (a longer time could not be used because of the significant decay of NKA control response under the present experimental settings). Agonist responses obtained with antagonist-treated cells were percentaged towards the time-matched control response, i.e. NKA induced PI response obtained in cells not treated with antagonists and that underwent the same number of washing cycles. Data indicate that receptor blockade exerted by the three antagonists is reversible although after a different number of washings (Figure 3). The inhibition exerted by nepadutant was quickly reverted: the NKA response after 3 washing periods (45 min) was the 90 ± 2% of time-matched control response. On the contrary, ibodutant and saredutant antagonism was reverted in a slower fashion: after 12 washing periods (180 min, as limit time of the experiment, see above) the NKA response in cells pretreated with saredutant and ibodutant was 91 ± 6% and 72 ± 4%, respectively, of the time-matched controls.

Ibodutant inhibition curves at the agonist and antagonist radioligand binding sites

Ibodutant completely inhibited the specific binding of all the three used radioligands, the agonist [^{125}I]NKA and the antagonists [^{3}H]nepadutant and [^{3}H]saredutant. K_d values calculated from homologous inhibition curves for NKA, nepadutant and saredutant, and K_i values calculated from ibodutant inhibition

Downloaded from jpet.aspetjournals.org at ASPET Journals on April 23, 2024

JPET Fast Forward. Published on February 13, 2009 as DOI: 10.1124/jpet.108.150201
This article has not been copyedited and formatted. The final version may differ from this version.

curves are reported in Table 1 (wild type receptor). Ibodutant displayed subnanomolar ihibitory affinity for the three radioligands. The fit of inhibition curves indicated different Hill slopes: not different from unity when evaluated towards [^{125}I]NKA and [^{3}H]nepadutant, the values being 0.87 (0.73 – 1.11, 95% c.l.) and 0.99 (0.81 – 1.18, 95% c.l.), respectively, whereas a slope significantly less than unity was measured by inhibition curves at the binding site of [^{3}H]saredutant (0.52, 0.43 – 0.60 95% c.l.).

To evaluate whether the competing ligand affinity was dependent on the time of incubation, and thus reflect non equilibrium conditions in the binding assay, inhibition curves with Ibodutant were conducted in a further set of experiments at the specific binding of [^{125}I]NKA by using different incubation periods: 30 min, 2 h, and 6 h. The total binding of [^{125}I]NKA did not change along the 6 h, thus indicating that no membrane/receptor degradation occurred. Ibodutant inhibition curves were superimposable and the calculated IC_{50} values did not differ (95% c.l.) being 0.07 nM (0.05 – 0.10) after 30 min, 0.04 nM (0.03 – 0.07) after 2 h, and 0.05 nM (0.04 – 0.06) after 6 h of incubation (n=3).

Ibodutant kinetic parameters determined by means of competition kinetic binding assay

Kinetic properties of ibodutant were evaluated by means of competition kinetic binding assay at the binding of the two antagonists nepadutant and saredutant which display different patterns of reversibility as also detected by different timing of recovery of funtional response (see above, Reversibility of tachykinin NK_2 receptor blockade).

Preliminary experiments were carried out to define the kinetic parameters (K_{obs}, observed association rate constant; K_{off}, dissociation rate constant) of [^{3}H]saredutant (K_{off} 0.043 ± 0.001 min^{-1}, K_{on} 4.85·10^{8} M^{-1} min^{-1}) and [^{3}H]nepadutant (K_{off} 0.13 ± 0.04 min^{-1}, K_{on} 1.13·10^{8} M^{-1} min^{-1}) (supplemental Figure 2).

Then we performed competition kinetic binding experiments to determine the K_{on} and K_{off} of the unlabeled ibodutant. Representative curves obtained are shown in Figure 4. Ibodutant was assayed at different concentrations towards the [^{3}H]nepadutant (Figure 4a) and the [^{3}H]saredutant (Figure 4b) binding association kinetic. No ligand depletion was evident under the present

Downloaded from jpet.aspetjournals.org at ASPET Journals on April 23, 2024

JPET Fast Forward. Published on February 13, 2009 as DOI: 10.1124/jpet.108.150201
This article has not been copyedited and formatted. The final version may differ from this version.

experimental conditions. The K_{on} value of ibodutant obtained in competition kinetic binding experiments towards [^{3}H]nepadutant was 1.15 ± 0.173 10^9 M^{-1} min^{-1}, and the K_{off} 0.055 ± 0.011 min^{-1}. The resulting (K_{off}/K_{on}) kinetic K_d was 0.050 ± 0.015 nM which agrees with the K_i value obtained through inhibition binding experiments at the [^{3}H]nepadutant binding site (K_i 0.07 nM, Table 1). The K_{on} value of ibodutant obtained in competition kinetic binding experiments using [^{3}H]saredutant as radioligand was 3.64 ± 2.50 10^8 M^{-1} min^{-1}, and the K_{off} 0.025 ± 0.008 min^{-1}. From these values a kinetic K_d of 0.175 ± 0.104 nM can be calculated which well matches the K_i value obtained in inhibition binding experiments at the [^{3}H]saredutant binding site (K_i 0.12 nM, Table 1).

Mutagenesis studies at the human tachykinin NK_2R to identify the binding site of ibodutant

In order to build experimental data to identify the binding site of ibodutant, its affinity was investigated at a number of 11 mutant receptors which were previously used to model the human tachykinin NK_2R interaction with nepadutant, saredutant (Giolitti *et al.*, 2000) and two structurally related antagonists of ibodutant (MEN13918 and MEN14268, Meini *et al.*, 2004). The investigated aminoacidic residues in the human tachykinin NK_2R sequence are schematically represented in Figure 5. C281Y (fourth extracellular loop) and I202F (TM4) were such mutated because these mutations spontaneously occur in the rat tachykinin NK_2R, and ibodutant displays low affinity for this species (Cialdai et al., 2006). C167G is a previously investigated mutation as responsible for tachykinin receptor subtype affinity and selectivity (Ciucci et al., 1997), whereas the other investigated mutated residues, all located in the transmembrane (TM) portion of the human tachykinin NK_2R sequence,
The affinity of ibodutant was evaluated in inhibiting the binding of [^{125}I]NKA, [^{3}H]nepadutant, and [^{3}H]saredutant, according to their capability to bind the single mutant receptors. The Hill slope values of fitting curves measured at the mutant receptors did not significantly differ from those measured at the wild type receptor (supplemental Table 1). The obtained results at each receptor in terms of K_d and K_i, as calculated by homologous and heterologous inhibition experiments, respectively (see Data analysis), are reported in Table 1. By the loss in affinity of ibodutant at the mutated receptors, as indicated by the F_{mut}

Downloaded from jpet.aspetjournals.org at ASPET Journals on April 23, 2024

JPET Fast Forward. Published on February 13, 2009 as DOI: 10.1124/jpet.108.150201
This article has not been copyedited and formatted. The final version may differ from this version.

index reported in Table 1, it results that receptor discriminants responsible for its high affinity at the tachykinin NK_2R are the C167 residue in TM4, I202 and Y206 in TM5, W263, Y266, and F270 in TM6, and Y289 in TM7 (Figure 5).
Results indicate that the binding site of ibodutant is in part overlapping to that of the agonist NKA and the antagonist nepadutant, comprised amongst TM4 (C167G), TM5 (Y206A), and TM6 (W263A, Y266F, F270A), but shares a determinant in TM7 (Y289F, Y289T) crucial for the binding of saredutant. Furthermore data obtained at the two mutants of Y289 in TM7 indicate a stronger dependency of ibodutant on the aromatic moiety of Y289 (greater reduction of affinity at the Y289T than at the Y289F mutant).
Moreover, in order to compare data obtained in the present study with those previously obtained with the close analogs of ibodutant, namely MEN13918 and MEN14268 (Meini et al., 2004, structures in Figure 6) the –log of F_{mut} values of the three antagonists have been plotted. Results indicate an overall similar profile of the three structurally related antagonists (Figure 6).

Molecular model of the human tachykinin NK_2R and ibodutant complex

The model of ibodutant docked to the human tachykinin NK_2R is shown in Figure 7. The model was reviewed according to experimental data obtained with mutant receptor. The pharmacophoric model indicated three hydrophobic parts represented by the benzothiophene, the cyclopentane and the D-phenylalanine moieties, and one positively charged group constituted by the amino group of the piperidine (Altamura et al., 2006). In the proposed docking model ibodutant occupies a binding pocket comprised among TMs 3, 4, 5, 6, and 7, the benzothiophenyl group being oriented toward C167 (TM4) to engage in a lipophilic interaction. The cyclopentyl group is packed between the I202 and the Y206 residues of TM5, whereas the adjacent D-phenylalanine sits in a cavity formed by aromatic residues in TM6 F270, Y266 and W263. This last residue is common to the sequences of the class A GPCRs, and its rotameric position is thought to be controlling the equilibrium between active and inactive states of the receptor. In this model the positive charge of the piperidinyl group finds a hydrogen bond counterpart in the hydroxyl group of Y289, and a lipophilic interaction between the Y289 and the tetrahydropyranyl group of ibodutant would further contribute to the stabilization of the ligand binding.

Downloaded from jpet.aspetjournals.org at ASPET Journals on April 23, 2024

JPET Fast Forward. Published on February 13, 2009 as DOI: 10.1124/jpet.108.150201
This article has not been copyedited and formatted. The final version may differ from this version.

Discussion

The present study focuses on the *in vitro* interaction properties of the nonpeptide antagonist ibodutant with the human tachykinin NK_2R with particular attention to its mechanism, kinetics and site of interaction.

We previously showed that ibodutant displays subnanomolar potency in antagonizing NKA induced contractions of human bladder smooth muscle (pK_B 9.2, Cialdai et al., 2006). In the present study, besides to confirm the subnanomolar antagonist potency of ibodutant for the recombinant human tachykinin NK_2R in the PI production (pK_B 10.3-10.6), its competitive antagonist behavior is defined by a complete Schild analysis (regression slope not significantly different from unity). Moreover, the comparison in the same assay with the two reference antagonists indicates that ibodutant is much more potent than nepadutant (pA_2 8.3) and slightly more potent than saredutant (pA_2 9.8). Potency values obtained with these two latter antagonists in this bioassay are in line with previous published results in different human tachykinin NK_2R assays, which reported for nepadutant and saredutant a surmountable and insurmountable antagonist mechanism, respectively (Patacchini et al., 2000; Catalioto et al., 1998b; Sellers et al., 2006; Advenier 1992; Huang et al., 1995). A critical aspect subjected to several reports and which regards the mechanism of GPCRs antagonists is the kinetic of receptor antagonism (Kenakin, 2006) and different approaches are exploited by investigators to characterize kinetic features of antagonists (Dowling and Charlton, 2006; Le et al., 2007; Lindström et al., 2007; Tian et al., 2007). In fact it is proposed that one of the most crucial factors for sustained drug efficacy *in vivo* is not the apparent affinity of the drug *per se*, but rather the residence time of the drug molecule on its molecular target, or in other words the period for which the receptor is occupied by the ligand; as a consequence it is conceived that a slow dissociating antagonist is likely to exert a longer efficient protection in vivo than a fast dissociating antagonist (Copeland et al., 2006; Vauquelin and Van Liefde, 2006). In the current investigation the kinetics of interaction of ibodutant were evaluated by using both a functional and radioligand binding experimental approach. We first evaluated antagonist dissociation and reversibility from the human NK_2R by using washout experiments, and we compared non-saturating concentrations of ibodutant with

Downloaded from jpet.aspetjournals.org at ASPET Journals on April 23, 2024

JPET Fast Forward. Published on February 13, 2009 as DOI: 10.1124/jpet.108.150201
This article has not been copyedited and formatted. The final version may differ from this version.

equieffective concentrations of nepadutant and saredutant. It appears that all the three antagonists can dissociate from the receptor although with a different time-course. Data obtained with nepadutant in this bioassay match quite well with those previously obtained in our laboratory by using the human colon smooth muscle contractility assay (Patacchini et al., 2000). On the contrary, a different behavior was observed with saredutant, which under the present experimental conditions did revert from receptor compartment although in a slower manner, whereas in the human smooth muscle assay the antagonist functional inhibition did rather increase despite the washout (Patacchini et al., 2000). Different experimental parameters may be responsible for this divergent behavior of saredutant in the two assays, such as the used agonist and antagonist concentrations, diffusion, and kinetic of the measured response (Patacchini et al., 2000; Giuliani et al., 1991; current study). In respect with ibodutant the presented results suggest that it does not act as an irreversible ligand but, similarly with saredutant, it dissociates rather slowly. Moreover, overlapping functional data obtained with ibodutant after different times of incubation (15 min versus 60 min) indicate that ibodutant easily attains equilibrium with the tachykinin NK_2R compartment. In agreement, the overlapping IC_{50} values obtained by means of ibodutant inhibition curves at the $[^{125}I]$NKA binding site, notwithstanding the increased time of incubation up to 6 hrs, support the concept that ibodutant associates with the receptor quite rapidly.

Ibodutant kinetics were also investigated by exploiting the competitive radioligand binding method (Motulsky and Mahan, 1984), as extensively reappraised by Dowling and Charlton (2006) to characterize the slow rate of dissociation of tiotropium, the anti-cholinergic drug of choice for the treatment of chronic obstructive pulmonary disease, from the M_3 muscarinic receptor. The current competition kinetic experiments were conducted with unlabelled ibodutant and the radiolabelled reference antagonists nepadutant and saredutant, with the advantage to compare the obtained results with structurally distinct antagonist radioligands. As discussed by Dowling and Charlton (2006), when the radioligand dissociates more rapidly than the competitor, the immediate radioligand binding is unaffected by the presence of the competitor, and the timing of the subsequent decline to equilibrium is related to the dissociation rate of unlabelled ligand, in our case ibodutant. Accordingly, results

Downloaded from jpet.aspetjournals.org at ASPET Journals on April 23, 2024

JPET Fast Forward. Published on February 13, 2009 as DOI: 10.1124/jpet.108.150201
This article has not been copyedited and formatted. The final version may differ from this version.

indicate that ibodutant dissociates more slowly than nepadutant, and at some extent also than saredutant, in agreement with results obtained from functional reversibility studies. The present evidence also points out that the kinetic parameters calculated for the competitor with this method largely depend on the chosen radioligand. In fact the kinetically derived constant affinity values ($K_d = K_{off} / K_{on}$) of ibodutant, calculated from the competition kinetics, well match those derived from heterologous competition experiments (K_i). In agreement, the dependency of constant affinity values on the used antagonist radioligand likewise reflects the different binding epitopes of nepadutant and saredutant (Giolitti et al., 2000; Almeida et al., 2004).

Thus in the second part of the study the binding recognition site of ibodutant has been investigated by using a panel of mutant NK_2Rs and radiolabelled [^{125}I]NKA, [^{3}H]nepadutant, and [^{3}H]saredutant depending on which radioligand was capable to bind the single mutants (Giolitti et al., 2000; Giolitti et al., 2002; Meini et al., 2004; Meini et al., 2005). We already showed that critical determinants for the binding of the peptide antagonist nepadutant were located in TMs 4, 5 and 6, whereas those responsible for the binding of the nonpeptide saredutant in TMs 6 and 7 (Giolitti et al., 2000). On the basis of mutagenesis combined with molecular modelling we hypothesize a model of ibodutant docked to the human tachykinin NK_2R and a binding pocket comprised among TMs 3, 4, 5, 6, and 7 (Figure 7). Such a quite extensive area identified in the receptor core involved in the binding site of ibodutant, may account for its high affinity detected at the NKA, nepadutant, and saredutant radioligands binding sites. Of particular interest is the supposed hydrophobic sandwich interaction between the D-phenylalanine moiety of ibodutant and a series of aromatic residues in TM6 which lie one helical turn one above the other, i.e. F270, 266 and 263. An important role for this tryptophan residue, which is commonly conserved amongst the sequences of the class A GPCRs, has been defined in controlling the equilibrium between active and inactive states of the receptor and is known as the “toggle switch”. In this switch, a rotameric change would let the movement of the cytoplasmic side of TM6 away from TM3 upon activation, thus permitting the opening of a cavity for G protein interaction and activation (Audet and Bouvier, 2008; Shukla et al., 2008). We speculate that the hydrophobic interactions between ibodutant D-phenylalanine moiety and TM6 aromatic

Downloaded from jpet.aspetjournals.org at ASPET Journals on April 23, 2024

JPET Fast Forward. Published on February 13, 2009 as DOI: 10.1124/jpet.108.150201
This article has not been copyedited and formatted. The final version may differ from this version.

residues can hinder the structural rearrangements necessary for activation and so constrain the receptor in an inactive state. This hypothesis is strengthened by the comparison of ibodutant with two analogs. As highlighted in the survey of results obtained with ibodutant and the previously presented MEN14268 and MEN13918 (Figure 6) their binding site is overlapping. We interpret the greater reduction of ibodutant and MEN13918 affinities as a different positioning of the D-phenylalanine moiety at a deeper level of TM6, which may be responsible for the higher affinity interaction and antagonist potency of these two ligands (ibodutant, $[^{125}I]$NKA binding: K_i 0.014 nM, current study, human urinary smooth muscle contractility pA_2 9.2, Cialdai et al., 2006; MEN13918: $[^{125}I]$NKA binding: K_i 0.2 nM, human urinary smooth muscle contractility pA_2 9.1, Meini et al., 2004), as compared to MEN14268 ($[^{125}I]$NKA binding: K_i 2.8 nM, human urinary smooth muscle contractility pA_2 8.3, Meini et al., 2004), and for the slow dissociation from the receptor compartment of ibodutant as measured in the present study. Altogether these findings support the notion that small ligands interact in a binding pocked in the transmembrane portion of GPCRs (Schwartz, 1994), but that the pocket itself can vary in position and orientation according to ligands and receptors specificity, as recently confirmed by crystallographic structures of the human β_2 adrenergic and A_{2A} adenosine receptors (Rasmussen et al., 2007; Rosenbaum et al., 2007; Jaakola et al., 2008).

Last, the drop in affinity measured with ibodutant at the I202F mutant, which spontaneously occurs in the rat tachykinin NK_2R, suggest that this residue could be largely responsible for the low affinity of ibodutant in the rat species (rat urinary bladder smooth muscle contractility pK_B 6.3, Cialdai et al., 2006) in agreement to what previously reported for this class of ligands (Meini et al., 2004).

In conclusion, the present study indicates that ibodutant displays fast associating and slow dissociating properties in the interaction with the human tachykinin NK_2R, and its reversibility from the receptor compartment. The analysis of ibodutant affinity at point-mutated receptors together with modeling let us to identify an antagonist binding pocket involving residues of TM3, 4, 5, 6, and 7, and to hypothesize an interaction model of this antagonist with the human tachykinin NK_2R.

Downloaded from jpet.aspetjournals.org at ASPET Journals on April 23, 2024

JPET Fast Forward. Published on February 13, 2009 as DOI: 10.1124/jpet.108.150201
This article has not been copyedited and formatted. The final version may differ from this version.

References

Advenier C, Rouissi N, Nguyen QT, Emonds-Alt X, Breliere JC, Neliat G, Naline E and Regoli D (1992) Neurokinin A (NK2) receptor revisited with SR 48968, a potent non-peptide antagonist. *Biochem Biophys Res Commun* **184:**1418-2144

Almeida TA, Rojo J, Nieto PM, Pinto FM, Hernandez M, Martín JD and Candenas ML (2004) Tachykinins and tachykinin receptors: structure and activity relationships. *Curr Med Chem* **11:**2045-2081.

Altamura M, Dapporto P, Fedi V, Giolitti A, Guerri A, Guidi A, Maggi CA, Paoli P and Rossi P (2006) New monocyclic and acyclic hNK-2 antagonists retaining the beta-turn feature. X-ray and molecular modelling studies. *Acta Crystallogr B* **62:**889-896.

Audet M and Bouvier M (2008) Insights into signaling from the beta2-adrenergic receptor structure. *Nat Chem Biol* **4:**397-403.

Catalioto RM, Criscuoli M, Cucchi P, Giachetti A, Gianotti D, Giuliani S, Lecci A, Lippi A, Patacchini R, Quartara L, Renzetti AR, Tramontana M, Arcamone F and Maggi CA (1998a) MEN 11420 (Nepadutant), a novel glycosylated bicyclic peptide tachykinin NK2 receptor antagonist. *Br J Pharmacol* **123:**81-91.

Catalioto RM, Cucchi P, Renzetti AR, Criscuoli M and Maggi CA (1998b) Independent coupling of the human tachykinin NK2 receptor to phospholipases C and A2 in transfected Chinese hamster ovary cells. *Naunyn Schmiedebergs Arch Pharmacol* **358:**395-403.

Cheng Y and Prusoff WH (1973) Relationship between the inhibition constant (K1) and the concentration of inhibitor which causes 50 per cent inhibition (I50) of an enzymatic reaction. *Biochem Pharmacol* **22:**3099-3108.

Cherezov V, Rosenbaum DM, Hanson MA, Rasmussen SG, Thian FS, Kobilka TS, Choi HJ, Kuhn P, Weis WI, Kobilka BK and Stevens RC (2007) High-resolution crystal structure of an engineered human beta2-adrenergic G protein-coupled receptor. *Science* **318:**1258-1265.

Cialdai C, Tramontana M, Patacchini R, Lecci A, Catalani C, Catalioto R-M, Meini S, Valenti C, Altamura M, Giuliani S and Maggi CA (2006) MEN15596, a

Downloaded from jpet.aspetjournals.org at ASPET Journals on April 23, 2024

JPET Fast Forward. Published on February 13, 2009 as DOI: 10.1124/jpet.108.150201
This article has not been copyedited and formatted. The final version may differ from this version.

novel nonpeptide tachykinin NK_2 receptor antagonist. *Eur J Pharmacol* **549:**140-148.

Ciucci A, Palma C, Riitano D, Manzini S and Werge TM (1997) Gly166 in the NK1 receptor regulates tachykinin selectivity and receptor conformation. *FEBS Lett* **416:**335-338.

Copeland RA, Pompliano DL and Meek TD (2006) Drug-target residence time and its implications for lead optimization. *Nat Rev Drug Discov* **5:**730-739.

Dowling MR and Charlton SJ (2006) Quantifying the association and dissociation rates of unlabelled antagonists at the muscarinic M_3 receptor. *Br J Pharmacol* **148:**927-937.

Emonds-Alt X, Golliot F, Pointeau P, Le Fur G and Breliere JC (1993) Characterization of the binding sites of [^{3}H]SR 48968, a potent nonpeptide radioligand antagonist of the neurokinin-2 receptor. *Biochem Biophys Res Comm* **191:**1172-1177.

Fedi V, Altamura M, Catalioto R-M, Giannotti D, Giolitti G, Giuliani S, Guidi A, Harmat NJS, Lecci A, Meini S, Nannicini R, Pasqui F, Tramontana M, Triolo A and Maggi CA (2007) Discovery of a new series of potent and selective linear tachykinin NK2 receptor antagonists. *J Med Chem* **50:**4793-4807.

Giolitti A, Cucchi P, Renzetti AR, Rotondaro L, Zappitelli S and Maggi CA (2000) Molecular determinantis of peptide and nonpeptide NK-2 receptor antagonists binding sites of the human tachykinin NK-2 receptor by site-directed mutagenesis. *Neuropharmacol* **39:**1422-1429.

Giolitti A, Altamura M, Bellucci F, Giannotti D, Meini S, Patacchini R, Rotondaro L, Zappitelli S and Maggi CA (2002) Monocyclic human tachykinin NK-2 receptor antagonists as evolution of a potent bicyclic antagonist: QSAR and site-directed mutagenesis studies. *J Med Chem* **45:**3418-3429.

Giuliani S, Altamura M and Maggi CA (2008) Ibodutant. *Drugs Fut* **33:**111-115.

Giuliani S, Barbanti G, Turini D, Quartara L, Rovero P, Giachetti A and Maggi CA (1991) NK_2 tachykinin receptors and contraction of circular muscle of the human colon: characterization of the NK_2 receptor subtype. *Eur J Pharmacol* **203:**365-370.

Huang RR, Vicario PP, Strader CD and Fong TM (1995) Identification of residues involved in ligand binding to the neurokinin-2 receptor. *Biochemistry* **34:**10048-10055.

Downloaded from jpet.aspetjournals.org at ASPET Journals on April 23, 2024

JPET Fast Forward. Published on February 13, 2009 as DOI: 10.1124/jpet.108.150201
This article has not been copyedited and formatted. The final version may differ from this version.

Jaakola VP, Griffith MT, Hanson MA, Cherezov V, Chien EY, Lane JR, Ijzerman AP and Stevens RC (2008) The 2.6 angstrom crystal structure of a human A2A adenosine receptor bound to an antagonist. *Science* **322:**1211-1217.

Kenakin TP (1997) Competitive antagonism. In: *Pharmacologic analysis of drug-receptor interaction.* 3rd ed. Lippincott-Raven Press Philadelphia. pp. 331-373.

Kenakin T, Jenkinson S and Watson C (2006) Determining the potency and molecular mechanism of action of insurmountable antagonists. *J Pharm Exp Ther* **319:**710-723.

Le MT, Pugsley MK, Vauquelin G and Van Liefde I (2007) Molecular characterisation of the interactions between olmesartan and telmisartan and the human angiotensin II AT1 receptor. *Br J Pharmacol* **151:**952-962.

Lecci A and Maggi CA (2003) Peripheral tachykinin receptors as potential therapeutic targets in visceral diseases. *Expert Opin Ther Targets* **7:**343-362.

Lindström E, von Mentzer B, Påhlman I, Ahlstedt I, Uvebrant A, Kristensson E, Martinsson R, Novén A, de Verdier J and Vauquelin G (2007) Neurokinin 1 receptor antagonists: correlation between in vitro receptor interaction and in vivo efficacy. *J Pharmacol Exp Ther* 322:1286-1293.

Meini S, Bellucci F, Catalani C, Cucchi P, Patacchini R, Rotondaro L, Altamura M, Giuliani S, Giolitti A and Maggi CA (2004) Mutagenesis at the human tachykinin NK_2 receptor to define the binding site of a novel class of antagonists. *Eur J Pharmacol* **488:**61-69.

Meini S, Catalani C, Bellucci F, Cucchi P, Giuliani S, Zappitelli S, Rotondaro L, Pasqui F, Guidi A, Altamura M, Giolitti A and Maggi CA (2005) Pharmacology of an original and selective nonpeptide antagonist ligand for the human tachykinin NK_2 receptor. *Eur J Pharmacol* **516:**104-111.

Motulsky HJ and Mahan LC (1984) The kinetics of competitive radioligand binding predicted by the law of mass action. *Mol Pharmacol* **25:**1-9.

Palczewski K, Kumasaka T, Hori T, Behnke CA, Motoshima H, Fox BA, Le Trong I, Teller DC, Okada T, Stenkamp RE, Yamamoto M and Miyano M (2000) Crystal structure of rhodopsin: A G protein-coupled receptor. *Science* **289:**739-745.

Patacchini P, Giuliani S, Turini A, Navarra G and Maggi CA (2000) Effect of nepadutant at tachykinin NK_2 receptors in human intestine and urinary bladder. *Eur J Pharmacol* **398:**389-397.

Downloaded from jpet.aspetjournals.org at ASPET Journals on April 23, 2024

JPET Fast Forward. Published on February 13, 2009 as DOI: 10.1124/jpet.108.150201
This article has not been copyedited and formatted. The final version may differ from this version.

Porcelloni M, D'Andrea P, Altamura M, Catalioto RM, Giuliani S, Meini S and Fattori D (2008) Cinnamic acids and mono-substituted benzoic acids as useful capping groups for the preparation of hNK2 receptor antagonists. *Bioorg Med Chem Lett.* **18:**4705-4707.

Quartara L and Altamura M (2006)Tachykinin receptors antagonists: from research to clinic. *Curr Drug Targets* **7:**975-992.

Renzetti AR, Catalioto R-M, Criscuoli M, Cucchi P, Lippi A, Guelfi M, Quartara L and Maggi CA (1998) Characterization of [^{3}H]MEN 11420, a novel glycosylated peptide antagonist radioligand of the tachykinin NK_2 receptor. *Biochem Biophys Res Comm* **248:**78-82.

Rasmussen SG, Choi HJ, Rosenbaum DM, Kobilka TS, Thian FS, Edwards PC, Burghammer M, Ratnala VR, Sanishvili R, Fischetti RF, Schertler GF, Weis WI and Kobilka BK (2007) Crystal structure of the human beta2 adrenergic G-protein-coupled receptor. *Nature* **450:**383-387.

Rosenbaum DM, Cherezov V, Hanson MA, Rasmussen SG, Thian FS, Kobilka TS, Choi HJ, Yao XJ, Weis WI, Stevens RC and Kobilka BK (2007) GPCR engineering yields high-resolution structural insights into beta2-adrenergic receptor function. *Science* **318:**1266-1273.

Schwartz TW (1994) Locating ligand-binding sites in 7TM receptors by protein engineering. *Curr Opin Biotechnol* **5:**434-444.

Sellers DJ, Chapple CR, Hay DPW and Chess-Williams R (2006) Depressed contractile responses to neurokinin A in idiopathic but not neurogenic overactive human detrusor muscle. *Eur Urol* **49:**510-518.

Shukla AK, Sun JP and Lefkowitz RJ (2008) Crystallizing thinking about the beta2-adrenergic receptor. *Mol Pharmacol* **73:**1333-1338.

Sisto A, Altamura M, Cardinali F, D'Andrea P, Rossi C and Fattori D (2007) α,α-Cyclic aminoacids as useful scaffolds for the preparation of hNK2 receptor antagonists. *Bioorg Med Chem Lett* **17:**4841-4844.

Tian G, Wilkins D and Scott CW (2007) Neurokinin-3 receptor-specific antagonists talnetant and osanetant show distinct mode of action in cellular Ca2+ mobilization but display similar binding kinetics and identical mechanism of binding in ligand cross-competition. *Mol Pharmacol* **71:**902-911.

Downloaded from jpet.aspetjournals.org at ASPET Journals on April 23, 2024

JPET Fast Forward. Published on February 13, 2009 as DOI: 10.1124/jpet.108.150201
This article has not been copyedited and formatted. The final version may differ from this version.

Vauquelin G and Van Liefde I (2006) Slow antagonist dissociation and long-lasting *in vivo* receptor protection. *Trends Pharmacol Sci* **27:**355-359

Downloaded from jpet.aspetjournals.org at ASPET Journals on April 23, 2024

JPET Fast Forward. Published on February 13, 2009 as DOI: 10.1124/jpet.108.150201
This article has not been copyedited and formatted. The final version may differ from this version.

Footnotes

Financial support for this project was in part provided by Italian Ministry of University and Research [4579]

Downloaded from jpet.aspetjournals.org at ASPET Journals on April 23, 2024

JPET Fast Forward. Published on February 13, 2009 as DOI: 10.1124/jpet.108.150201
This article has not been copyedited and formatted. The final version may differ from this version.

Legends for Figures

Fig. 1.

Ibodutant antagonism on NKA-induced PI accumulation. **a**: concentration-response curves to NKA in the absence (control) or presence of the indicated concentration of ibodutant in the legend; in the x axys the log of NKA concentrations are indicated; the PI accumulation is indicated in the y axys as percentage of the control maximal effect (E_{max}). Cells were incubated with NKA for 30 min at 37°C as described under Methods. Ibodutant (0.3, 1, 3, 10, or 30 nM) was preincubated 15 min before the agonist administration. **b**: Schild regression of ibodutant antagonism: the antagonist concentrations (x axys) are plotted against the log (CR – 1). Data points are expressed as mean ± s.e.mean of 3-4 experiments

Fig. 2.

Nepadutant and saredutant antagonism on NKA-induced PI accumulation. Cells were incubated with NKA for 30 min at 37°C as described under Methods. Nepadutant (**a**, 100 nM, 1 µM) or saredutant (**b**, 3, 30 nM) were preincubated 15 min before the administration of concentration-response curves to NKA. PI accumulation is indicated in the y axys as percentage of the control maximal effect (E_{max}). Data points are expressed as mean ± s.e.mean of 3 experiments.

Fig. 3.

Reversibility of human tachykinin receptor blockade induced by nepadutant, saredutant, and ibodutant in the PI accumulation assay. Cells were incubated 15 min with antagonists at 37°C as described under Methods, then responses to NKA (30 nM incubated for 30 min) were obtained, immediately or after different wash period during which the medium was renewed (one wash period was 15 min, x axys). Data were percentaged towards control time-matched responses. Data are expressed as mean ± s.e.mean of 3 experiments, each one performed in triplicate.

Downloaded from jpet.aspetjournals.org at ASPET Journals on April 23, 2024

JPET Fast Forward. Published on February 13, 2009 as DOI: 10.1124/jpet.108.150201
This article has not been copyedited and formatted. The final version may differ from this version.

Fig. 4.

[^{3}H]nepadutant (a) and [^{3}H]saredutant (b) competition kinetics curves in the presence of ibodutant. Membranes (100 µg/ml) of CHO cell expressing the human tachykinin NK_2R were incubated with [^{3}H]nepadutant (1-1.3 nM), or [^{3}H]saredutant (2.5 - 3 nM), and the indicated concentrations of ibodutant for the indicated time (x axes, a: 0-360 min). Data were fitted with the equations described by Dowling and Charlton (2006) to calculate K_{on} and K_{off} values for ibodutant. Data are representative of 3-4 experiments, and are expressed as mean ± s.e.m. Determination were performed in triplicate.

Fig. 5.

Schematic representation of human tachykinin NK_2 receptor.
The alignment of the helical regions of the receptor is based on conserved residues present throughout the GPCR class A (rhodopsin-like). Aminoacidic residues which have been investigated by site-directed mutagenesis in this study are bold circled and numbered (Q109, C167, T171, I202, Y206, W263, Y266, F270, C281, Y289), and those involved in the putative binding site of ibodutant are in white-on-shaded in grey (C167, Y206, W263, Y266, F270, Y289). The I202F mutation spontaneously occurs in the sequence of the rat/mouse tachykinin NK_2 receptor is suggested to hamper the proper interaction of ibodutant with residues located at a deeper level in the transmembrane (TM) portion. Mutations which abrogate the NKA binding: C167G, Y206A, W263A, F270A, Y289T; mutations which abrogate the nepadutant binding: C167G, T171A, Y206A, W263A, Y266F, F270A; mutations which abrogate the saredutant binding: Y289F, Y289T.

Fig. 6.

Comparison of the effects of point mutations at the human tachykinin NK_2 receptors on the affinity of ibodutant, MEN13918, and MEN14268. F_{mut} [K_i(mutant receptor)/K_i(wild type receptor)] have been transformed to log and plotted according to the used radioligand: a: [^{125}I]neurokinin A, b: [^{3}H]nepadutant, c: [^{3}H]saredutant. Data obtained with Ibodutant are from the present study (Table

Downloaded from jpet.aspetjournals.org at ASPET Journals on April 23, 2024

JPET Fast Forward. Published on February 13, 2009 as DOI: 10.1124/jpet.108.150201
This article has not been copyedited and formatted. The final version may differ from this version.

1), whereas data referred to MEN13918 and MEN14268 are from Meini *et al.*, 2004.

Fig. 7.

Proposed docking mode of ibodutant with the human tachykinin NK_2R. Views from the transmembrane (a) and extracellular (b) side. Investigated residues supposed to interact with ibodutant are differently coloured depending on the TM location and numbered. The docking solution selected is consistent with experimental data obtained through site-directed mutagenesis described in the current work. The benzothiophenyl group of ibodutant interacts with C167 (TM4) through lipophilic interaction, the cyclopentyl moiety with the I202 and Y206 (TM5) residues, the phenylalanine residue trapped amongst F270, Y266, and W263 (TM6), and a hydrogen bond between the piperidine nitrogen of ibodutant and the hydroxylic function of Y289 (TM7).

Downloaded from jpet.aspetjournals.org at ASPET Journals on April 23, 2024

Table 1

Ligand binding affinity values measured at wild type and mutant human tachykinin NK_2 receptors

	$[^{125}I]$neurokinin A nM (95% c.l.)			$[^{3}H]$nepadutant nM (95% c.l.)			$[^{3}H]$saredutant nM (95% c.l.)		
	neurokinin A K_d	**ibodutant** K_i	F_{mut}	**nepadutant** K_d	**ibodutant** K_i	F_{mut}	**saredutant** K_d	**ibodutant** K_i	F_{mut}
wild type	1.3 (0.8 - 2.2)	0.014 (0.010 - 0.017)	1	2.1 (1.1 - 4.1)	0.07 (0.054 - 0.083)	1	0.3 (0.2 - 0.5)	0.12 (0.079 - 0.194)	1
Q109A	2.3 (1.5 - 3.4)	0.03 (0.02 - 0.04)	2.1	1.7 (1.4 - 2.04)	0.09 (0.07 - 0.1)	1.3	0.99 (0.8 - 1.2)	0.05 (0.04 - 0.06)	0.4
C167G	n.d.b.			n.d.b.			3.7 (1.7 - 7.8)	33.8 (23.1 - 49.8)	**282**
T171A	0.8 (0.5 - 1.1)	0.015 (0.012 - 0.019)	1.1	n.d.b.			0.3 (0.2 - 0.6)	0.2 (0.2 - 0.3)	1.7
I202F	1.9 (1.4 - 2.5)	5.4 (4.5 - 6.5)	**386**	0.5 (0.3 - 0.8)	9.01 (7.7 - 10.5)	**129**	0.3 (0.2 - 0.4)	13.4 (11.6 - 16.01)	**112**
Y206A	n.d.b.			n.d.b.			3.7 (2.4 - 5.8)	6.6 (4.1 - 10.5)	**55**
W263A	n.d.b.			n.d.b.			5.4 (2.7 - 10.8)	20.1 (12 - 33.4)	**168**
Y266F	1.04 (0.85 -1.3)	0.6 (0.5 - 0.8)	**43**	n.d.b.			2.2 (1.5 -3.4)	2.5 (1.98 - 3.2)	**21**
F270A	n.d.b.			n.d.b.			1.3 (0.9 - 1.9)	7.9 (6.2 - 10.04)	**66**
C281Y	0.8 (0.6 - 0.9)	0.02 (0.02 - 0.03)	1.4	3.16 (1.77 - 5.58	0.053 (0.03 - 0.095)	0.8	0.5 (0.4 - 0.7)	0.35 (0.3 - 0.4)	2.9
Y289F	1.07 (0.86 - 1.3	0.4 (0.3 - 0.5)	**29**	3.84 (2.68 - 5.49	0.7 (0.47 - 1.04)	**10**	n.d.b.		
Y289T	n.d.b.			16 (8 - 31)	24.3 (16.8 - 35.2)	**347**	n.d.b.		

Experiments were carried out on membrane preparations from pooled clones of CHO cells stably expressing the wild type or mutant human tackykinin NK_2 receptors, by using the peptide agonist $[^{125}I]$NKA, the cyclic peptide antagonist $[^{3}H]$nepadutant, and the nonpeptide antagonist $[^{3}H]$saredutant as radioligands, as described under Methods. Radioligands K_d constant affinity values were calculated by means of homologous inhibition experiments and expressed in nM concentration, for each receptor. K_i values of the

JPET Fast Forward. Published on February 13, 2009 as DOI: 10.1124/jpet.108.150201
This article has not been copyedited and formatted. The final version may differ from this version.

Downloaded from jpet.aspetjournals.org at ASPET Journals on April 23, 2024

competing ligand ibodutant (in nM concentration) were calculated from heterologous inhibition experiments according to the concentration and K_d of the used radioligand for each mutant receptor (See Methods). F_{mut} is calculated as K_i(mutant receptor)/K_i(wild type human tachykinin NK_2 receptor), and refers to fold decrease in the affinity of ibodutant. Significant decreases in affinity are indicated by F_{mut} indexes in bold. K_d and K_i values are expressed as mean and 95% confidence limits in parenthesis of 3 experiments, each one performed in duplicate. n.d.b. not detectable binding.

JPET Fast Forward. Published on February 13, 2009 as DOI: 10.1124/jpet.108.150201
This article has not been copyedited and formatted. The final version may differ from this version.

Downloaded from jpet.aspetjournals.org at ASPET Journals on April 23, 2024

Fig.1

a

PI accumulation (% of control E_{max})

100

50

0

-11 -10 -9 -8 -7 -6 -5 -4

log [NKA] M

control

ibodutant:

0.3 nM

3 nM

30 nM

b

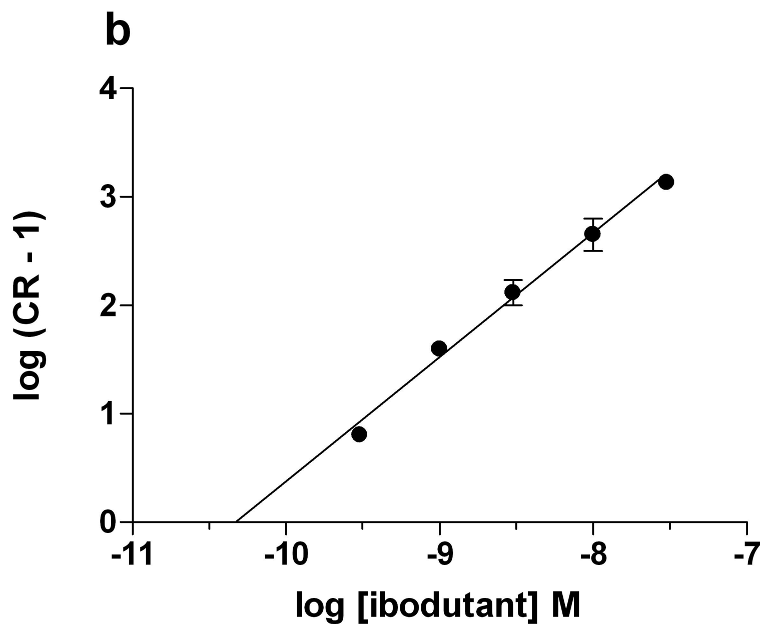

Fig. 2

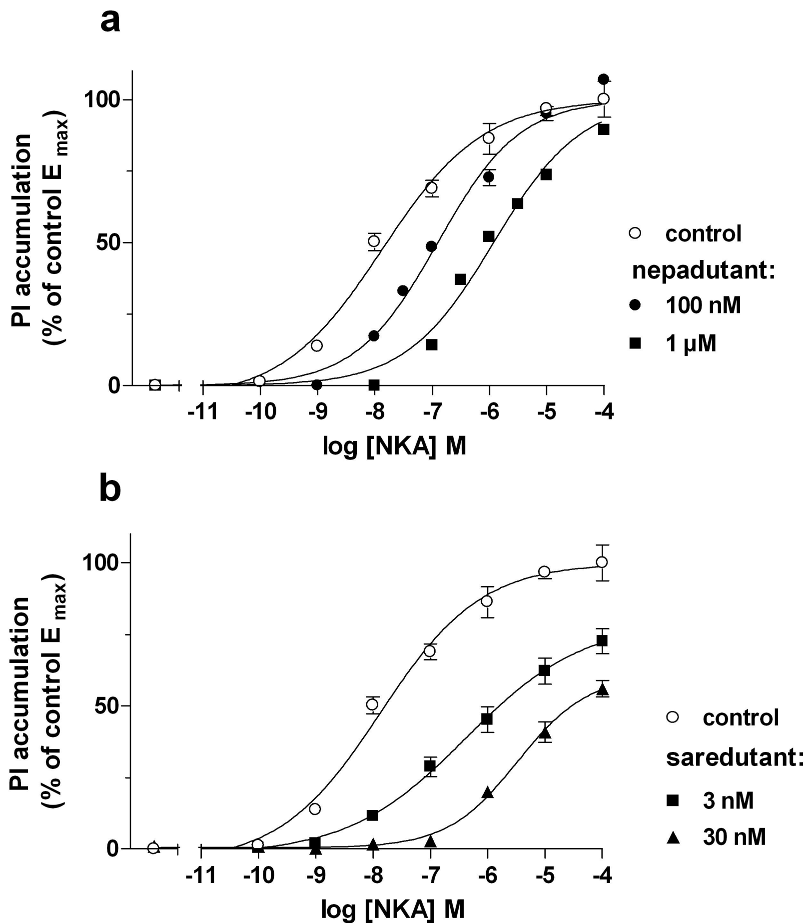

Fig. 3

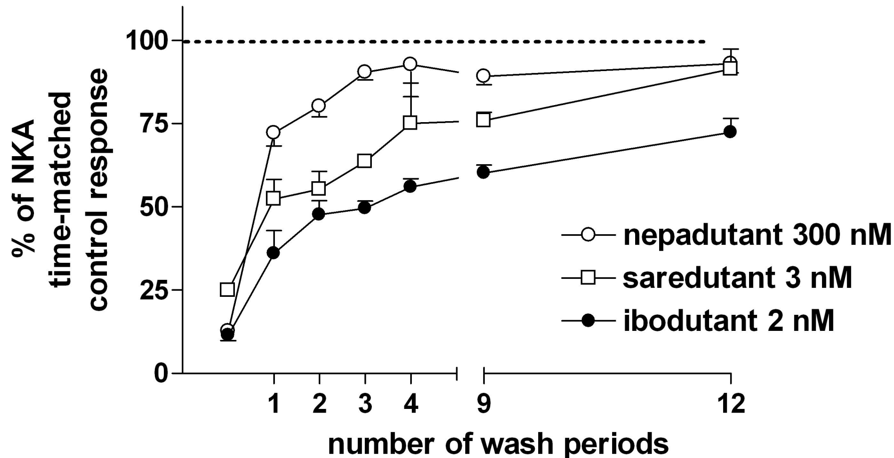

JPET Fast Forward. Published on February 13, 2009 as DOI: 10.1124/jpet.108.150201
This article has not been copyedited and formatted. The final version may differ from this version.

Fig. 4

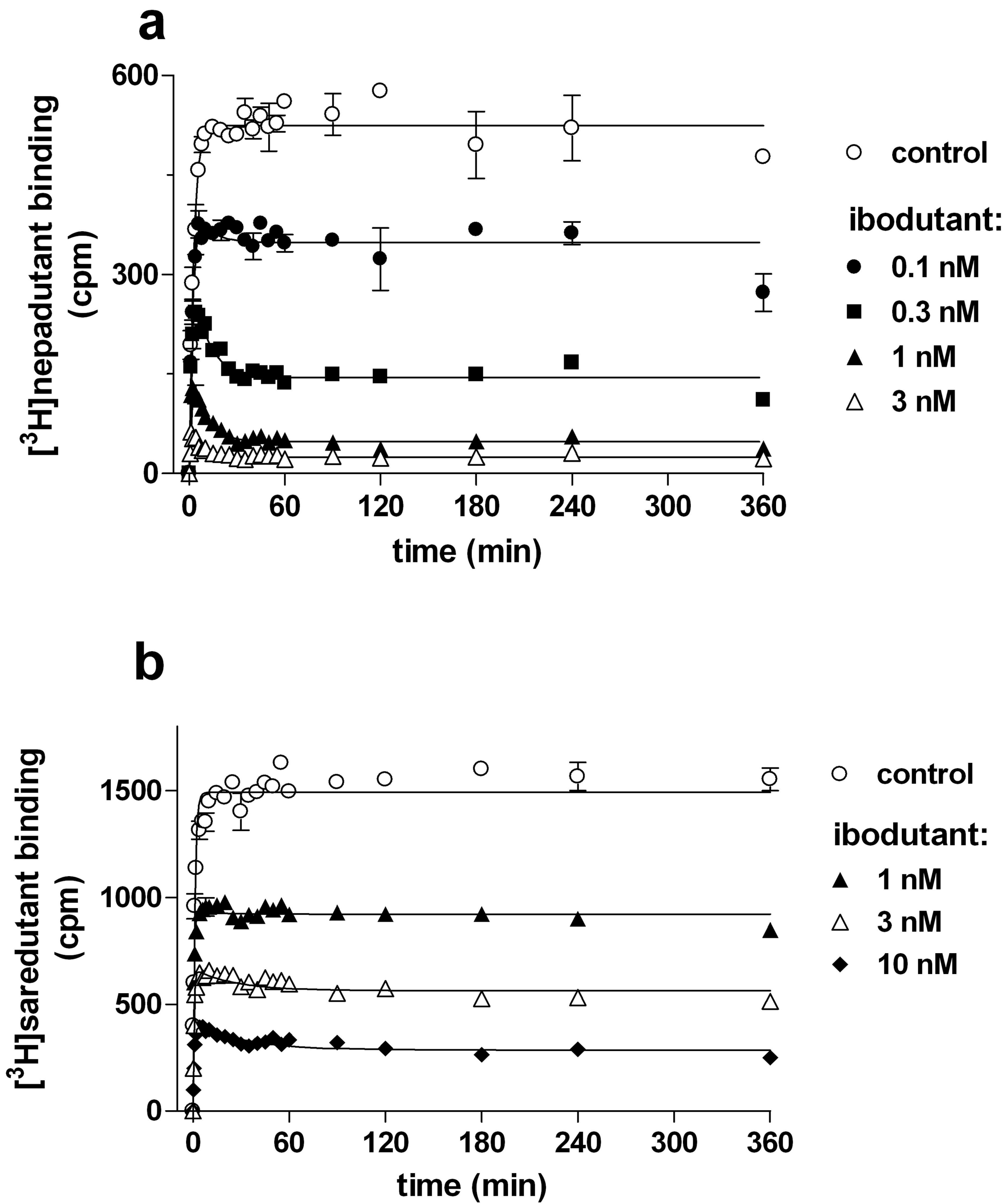

Downloaded from jpet.aspetjournals.org at ASPET Journals on April 23, 2024

JPET Fast Forward. Published on February 13, 2009 as DOI: 10.1124/jpet.108.150201
This article has not been copyedited and formatted. The final version may differ from this version.

Fig. 5

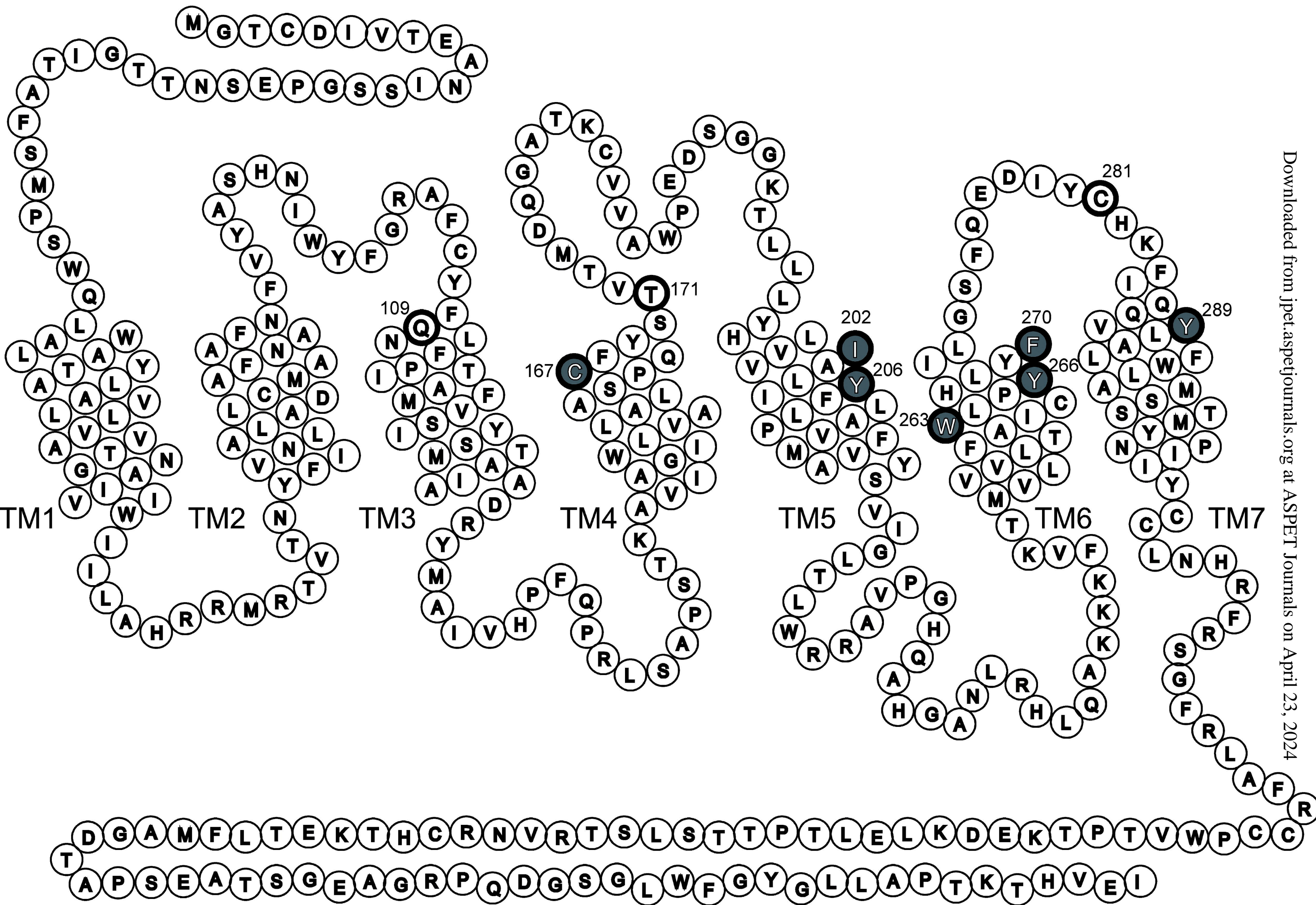

Downloaded from jpet.aspetjournals.org at ASPET Journals on April 23, 2024

Fig. 6

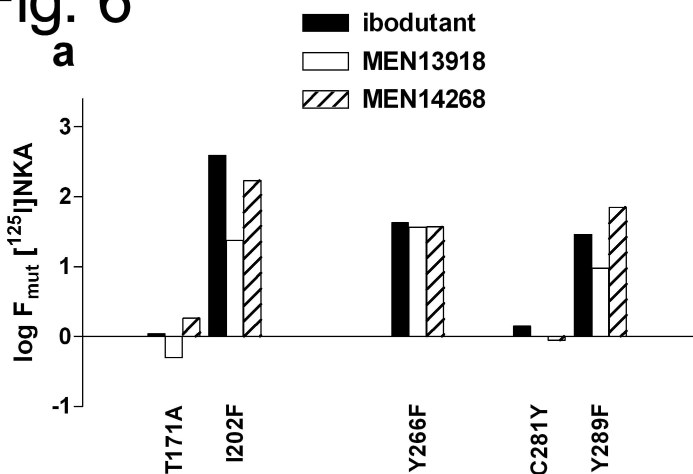

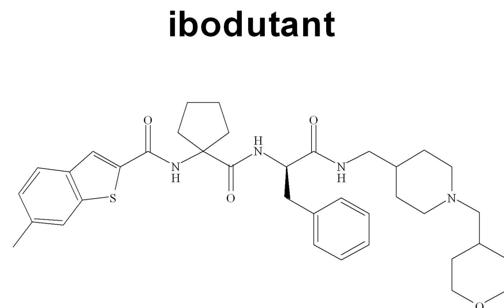

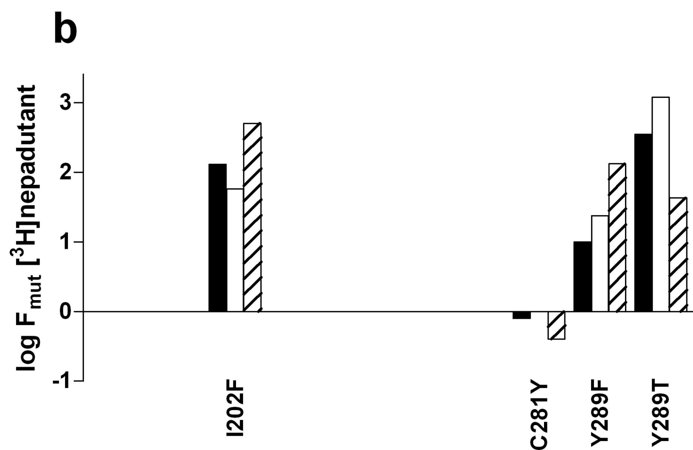

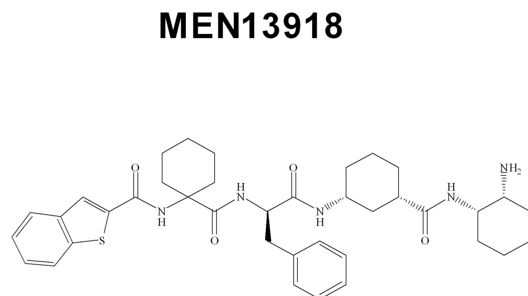

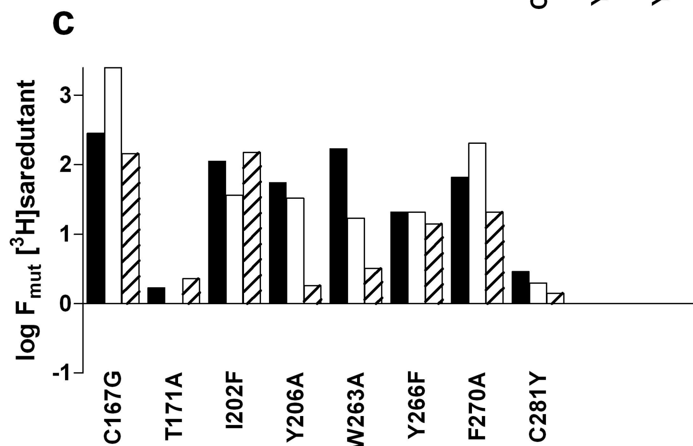

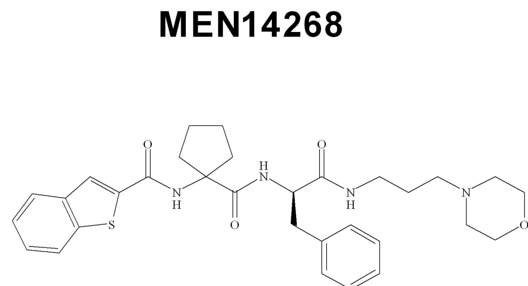

Fig.7

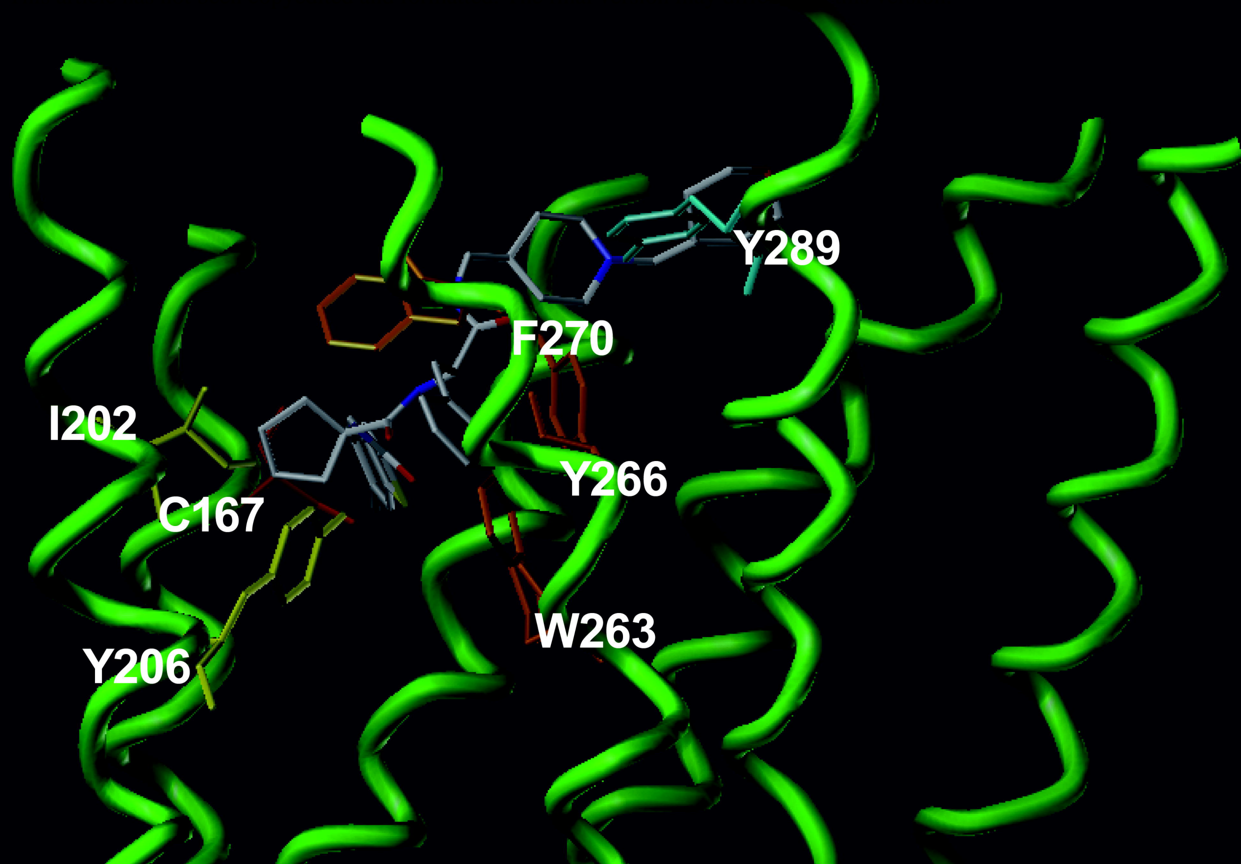

b
TM4
TM2
C167
TM3
I202
TM1
Y206
TM7
W263
TM5
F270
Y289
Y266
TM6